In-flight dissipation as a mechanism to suppress Fermi acceleration

Diego F. M. Oliveira and Marko Robnik
CAMTP–Center For Applied Mathematics and Theoretical Physics, University of Maribor, Krekova 2, SI-2000 Maribor, Slovenia
(Received 1 November 2010; published 14 February 2011)

Some dynamical properties of time-dependent driven elliptical-shaped billiards are studied. It was shown that for conservative time-dependent dynamics the model exhibits Fermi acceleration [Phys. Rev. Lett. **100**, 014103 (2008).] On the other hand, it was observed that damping coefficients upon collisions suppress such a phenomenon [Phys. Rev. Lett. **104**, 224101 (2010)]. Here, we consider a dissipative model under the presence of in-flight dissipation due to a drag force which is assumed to be proportional to the square of the velocity of the particle. Our results reinforce that dissipation leads to a phase transition from unlimited to limited energy growth. The behavior of the average velocity is described using scaling arguments.

DOI: 10.1103/PhysRevE.83.026202 PACS number(s): 05.45.Ac, 05.45.Pq

I. INTRODUCTION

Dissipative systems have attracted much attention during the last few years since they can be used to explain different physical phenomena in different fields of science, including atomic and molecular physics [1,2], turbulent and fluid dynamics [3–5], optics [6,7], nanotechnology [8,9], and quantum and relativistic systems [10,11]. Different procedures can be used to describe such systems. Billiard models are often considered since they can easily be described mathematically and can be realized experimentally in many different ways; for example, by using microwave resonators, as initiated by Stöckmann in 1990 [12], and as well as by using superconducting microwave resonators [13], quantum dots [14], and ultracold atoms [15], along with many others. From a mathematical point of view, a billiard is defined by a connected region, $Q \subset R^D$, with a boundary $\partial Q \subset R^{D-1}$ which separates Q from its complement. If the system has a time-dependent boundary, $\partial Q = \partial Q(t)$, it can exchange energy with the particle upon collision. In such a case, it is possible to investigate the phenomenon called Fermi acceleration, i.e., unlimited energy growth [16]. According to the Loskutov-Ryabov-Akinshin (LRA) conjecture [17], a chaotic component in phase space with a static boundary is a sufficient condition to observe Fermi acceleration when a time-dependent perturbation is introduced. Results that corroborate the validity of this conjecture include the time-dependent oval billiard [18], stadium billiard [19], and Lorentz gas [20]. Recently, it was shown even that a specific perturbation in the boundary of an elliptical billiard (integrable) leads to unlimited energy growth [21]. The separatix gives place to a chaotic layer and the particles can now experience unlimited energy growth while diffusing in the chaotic layer.

The paper is organized as follows. In Sec. II we describe the details in order to obtain the four-dimensional mapping which describes the dynamics of the system. Section III is devoted to the numerical results. Conclusions are drawn in Sec. IV.

II. MODEL AND MAP

In this paper, we will consider a dissipative elliptical billiard with a periodically moving boundary as has been studied in the pioneering paper in 1996 [22]. Usually, dissipation is considered upon collision when damping coefficients (see Refs. [23,24] and references therein) or dissipation during flight are introduced [25–27]. First, we assume that particles of mass m are immersed in a fluid. The dissipative drag force is considered to be proportional to the square of the velocity of the particle, $\vec{V}$. In Ref. [28], collisional dissipation is considered and in Ref. [29] viscous drag force (in-flight dissipation) is shown. Both studies found the suppression of Fermi acceleration, but neither of them considered the acceleration exponents. To obtain the equation that describes the velocity of the particle along its trajectory, we need to solve Newton's equation, where $md|\vec{V}|/dt = -\eta' \vec{V}^2$ with the initial velocity $|\vec{V}_n| > 0$, and where η' is the coefficient of the drag force. After we introduce the variables $\eta'/m = \eta$, we obtain the velocity of the particle as function of time as $\vec{V}_p(t) = \vec{V}_n/[1 + V_n\eta(t - t_n)]$, where $V_n = |\vec{V}_n|$. We describe the model using a four-dimensional nonlinear map, $T(\theta_n,\alpha_n,|\vec{V}_n|,t_n) = (\theta_{n+1},\alpha_{n+1},|\vec{V}_{n+1}|,t_{n+1})$, where the dynamical variables are, respectively, the angular position of the particle, the angle formed by the trajectory of the particle with the tangent line at the position of the collision, the absolute velocity of the particle, and the instant of the hit with the boundary. Figure 1 illustrates the geometry of five successive collisions of the particle with the time-dependent boundary. To obtain the map, we start with an initial condition $(\theta_n,\alpha_n,|\vec{V}_n|,t_n)$. The Cartesian components of the boundary at the angular position (θ_n,t_n) are the following:

$$X(\theta_n,t_n) = [A_0 + C\sin(t_n)]\cos(\theta_n), \quad (1)$$

$$Y(\theta_n,t_n) = [B_0 + C\sin(t_n)]\sin(\theta_n), \quad (2)$$

where A_0 and B_0 are constants. Thus at any time, t_n, we have an elliptical shape. The control parameter $0 < C < \min(A_0,B_0)$ controls the amplitude of oscillation and $\theta \in [0,2\pi)$ is a counterclockwise polar angle measured with respect to the positive horizontal axis. The angle between the tangent of the boundary at the position $[X(\theta_n),Y(\theta_n)]$ measured with respect to the horizontal line is $\tan(\phi_n) = (\frac{(Y'(\theta_n,t_n)}{X'(\theta_n,t_n))})$, where $X'(\theta_n,t_n) = dX(\theta_n,t_n)/d\theta_n$ and $Y'(\theta_n,t_n) = dY(\theta_n,t_n)/d\theta_n$. Since the expressions for ϕ_n and α_n are known, the angle of the trajectory of the particle measured with respect to the positive X axis is $(\phi_n + \alpha_n)$. Such information allows us to write the particle's velocity vector as $\vec{V}_n = |\vec{V}_p(t)|[\cos(\phi_n + \alpha_n)\hat{i} + \sin(\phi_n + \alpha_n)\hat{j}]$, where $\hat{i}$ and $\hat{j}$ denote

 ©2011 American Physical Society

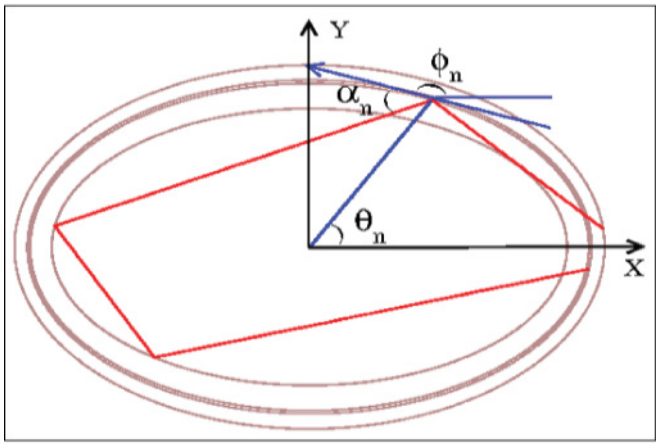

FIG. 1. (Color online) Illustration of the five collisions with a time-dependent boundary. The corresponding angles describing the dynamics are also illustrated.

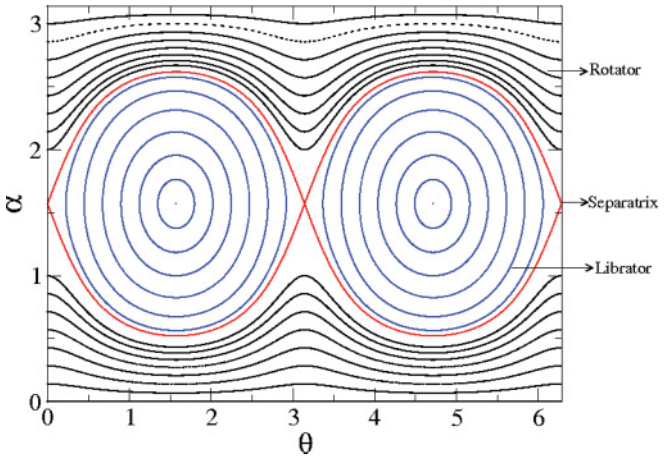

FIG. 2. (Color online) Phase space for the static elliptical billiard. The control parameters are denoted as $A_0 = 2$ and $B_0 = 1$.

the unity vectors with respect to the X and Y axes, respectively. The particle travels on a straight line until it hits the time-dependent boundary. The position of the particle, as a function of time, for $t \geqslant t_n$, is $X_p(t) = X(\theta_n,t_n) + r(t)\cos(\phi_n + \alpha_n)$, $Y_p(t) = Y(\theta_n,t_n) + r(t)\sin(\phi_n + \alpha_n)$, where the subindex p denotes that such coordinates correspond to the particle and $r(t) = \eta^{-1}\ln[1 + V_n\eta(t - t_n)]$, which is the displacement of the particle obtained from direct integration of $dr(t)/dt = |\vec{V}_p(t)|$. The distance of the particle measured with respect to the origin of the coordinate system is given by $R_p(t) = \sqrt{X_p^2(t) + Y_p^2(t)}$, and θ_p at $X_p(t),Y_p(t)$ is $\theta_p = \arctan[Y_p(t)/X_p(t)]$. Therefore, the angular position at the $(n + 1)$th collision of the particle with the boundary, i.e., θ_{n+1}, is numerically obtained by solving the following equation: $R_p(t) = \sqrt{X^2(\theta_p,t) + Y^2(\theta_p,t)}$. We use the bisection method to numerically solve this equation. The time at the $(n + 1)$th collision is obtained by evaluating $t_{n+1} = t = t_n + t_c$, where t_c is the time during the flight. To obtain this new velocity we should note that the reference frame of the boundary continues to move. Therefore, at the instant of collision, the following conditions must be obeyed:

$$\vec{V}_{n+1} \cdot \vec{T}_{n+1} = \vec{V}_n \cdot \vec{T}_{n+1}, \tag{3}$$

$$\vec{V}_{n+1} \cdot \vec{N}_{n+1} = -\vec{V}_n \cdot \vec{N}_{n+1} + 2\vec{V}_b(t_{n+1}) \cdot \vec{N}_{n+1}, \tag{4}$$

where $\vec{T}$ and $\vec{N}$ are the unitary tangent and normal vectors, respectively, and the velocity of the boundary is $\vec{V}_b(t_{n+1}) = C\cos(t_{n+1})\,[\cos(\theta_{n+1})\hat{i} + \sin(\theta_{n+1})\hat{j}]$. Then we have

$$|\vec{V}_{n+1}| = \sqrt{(\vec{V}_{n+1} \cdot \vec{T}_{n+1})^2 + (\vec{V}_{n+1} \cdot \vec{N}_{n+1})^2}. \tag{5}$$

Finally, the angle α_{n+1} is written as

$$\tan(\alpha_{n+1}) = \left(\frac{\vec{V}_{n+1} \cdot \vec{N}_{n+1}}{\vec{V}_{n+1} \cdot \vec{T}_{n+1}}\right). \tag{6}$$

With this four-dimensional mapping, we can explore the dynamics of the model. However, before considering the time-dependent model, let us illustrate the behavior of the phase space for the static boundary. Indeed, it is well known that the ellipse is an integrable billiard system, the product of the two angular momenta with respect to the foci being the integral of motion [30,31]. Figure 2 shows the phase space for $A_0 = 2$ and $B_0 = 1$. We can see a large double island limited by a separatrix and a set of invariant spanning curves. We can observe two types of behavior separated by a separatrix (red curve), namely, rotators and librators. Librators consist of trajectories that are confined between the two foci and in the phase space are confined by the separatrix curve. On the other hand, rotators are trajectories near the boundary that explore all the values of θ. In phase space they are outside of the separatrix curve.

III. NUMERICAL RESULTS

As a part of our numerical results, in the following we will mainly discuss the behavior of the average velocity of the particle. Two steps were applied in order to obtain the average velocity. First, we evaluate the average velocity over the orbit for a single initial condition (fixed i) and then over an ensemble of initial conditions. This procedure is motivated by the fact that phase space is four dimensional and it is difficult and perhaps even meaningless to study typical orbits individually. Hence, the average velocity is written as

$$\overline{V} = \frac{1}{M}\sum_{i=1}^{M}\frac{1}{n+1}\sum_{j=0}^{n} V_{i,j}, \tag{7}$$

where the index i denotes a member of an ensemble of initial conditions, and M is the number of different initial conditions. We have considered $M = 200$ in our simulations. It was shown by Lenz *et al.* [21,32] that when a driving perturbation is introduced into the system, opposite to expectations, it exhibits a phenomenon known as Fermi acceleration or unlimited energy gain. Such a behavior happens when the driving amplitude $C \neq 0$ and the separatix is replaced by a chaotic layer. A particle which starts its dynamics in a rotator orbit can change its dynamics to a librator and vice versa. The chaotic diffusion within the chaotic layer leads to unlimited energy growth. Figure 3 shows the behavior of the average velocity as a function of the number of collisions. We have considered the nondissipative case where the drag coefficient is $\eta = 0$. This is

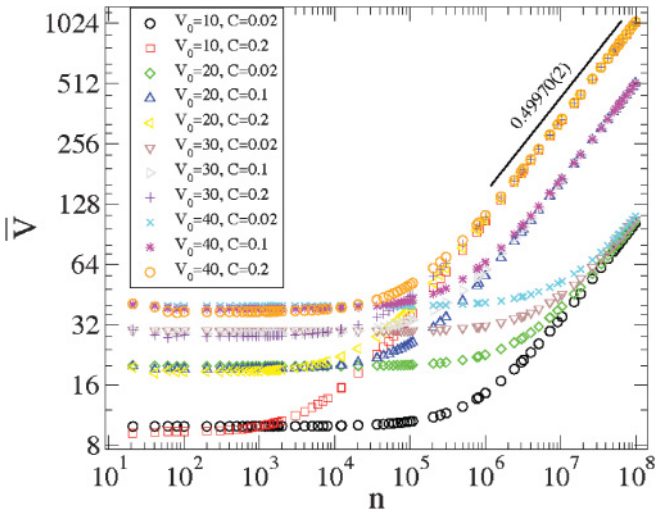

FIG. 3. (Color online) Behavior of $\bar{V}$ vs n for different initial velocities. The control parameters used were $A_0 = 2$ and $B_0 = 1$. This is the nondissipative case with vanishing drag force $\eta = 0$.

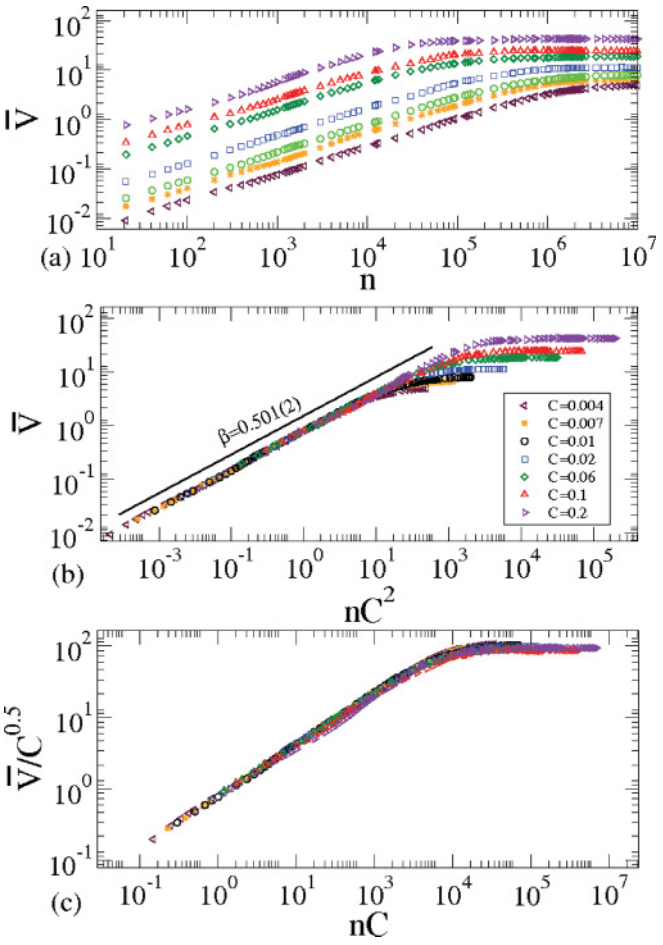

FIG. 4. (Color online) (a) Behavior of the average velocity as a function of n for different values of the control parameter C. (b) The initial collapse after the transformation nC^2. (c) The collapse onto a single universal plot.

a time-dependent Hamiltonian system in which the Liouville theorem of phase-space volume conservation still applies. For such a case, the velocity of the particle is $\vec{V}_p(t) = \vec{V}_n$ and $r(t) = V_n(t - t_n)$. As one can see, all the curves of $\bar{V}$ behave quite similarly in the sense that (a) for short $n \ll n_x$, the average velocity remains constant for a while up to $n \approx n_x$, but eventually, after a crossover (b) $n \approx n_x$, all the curves start growing with the same exponent at $n \gg n_x$. This is in agreement with the results obtained by Lenz *et al.* [33,34], where they consider the average velocity for large enough values of n.

We now discuss the effect of dissipation introduced via a frictional force. To obtain the average velocity, we randomly choose $t \in [0,2\pi]$, $\theta \in [0,2\pi]$, and $\alpha \in [0,\pi]$. We also fix the value of $\eta = 10^{-3}$. Additionally, in order to avoid the initial plateau we also have fixed the initial velocity as $V_0 = 10^{-5}$. The model of collisional dissipation by Leonel and Bunimovich [28] is different from our model of in-flight dissipation due to the drag force in detail, but it should behave similarly in the statistical sense (on the average), especially in the chaotic regime because then we have $\langle V_{n+1}\rangle = \langle V_n\rangle e^{-\eta r}$. Thus the effective damping coefficient is $\delta = e^{-\eta\langle r\rangle}$, where $\langle r\rangle$ is the mean-free path of the particle.

In Fig. 4(a) we show the behavior of the average velocity as a function of the number of collisions for different values of C. Note that for different values of C and for short n, the average velocity starts to grow and then it bends toward a regime of saturation for long enough values of n. It must be emphasized that different values of the parameter C generate different

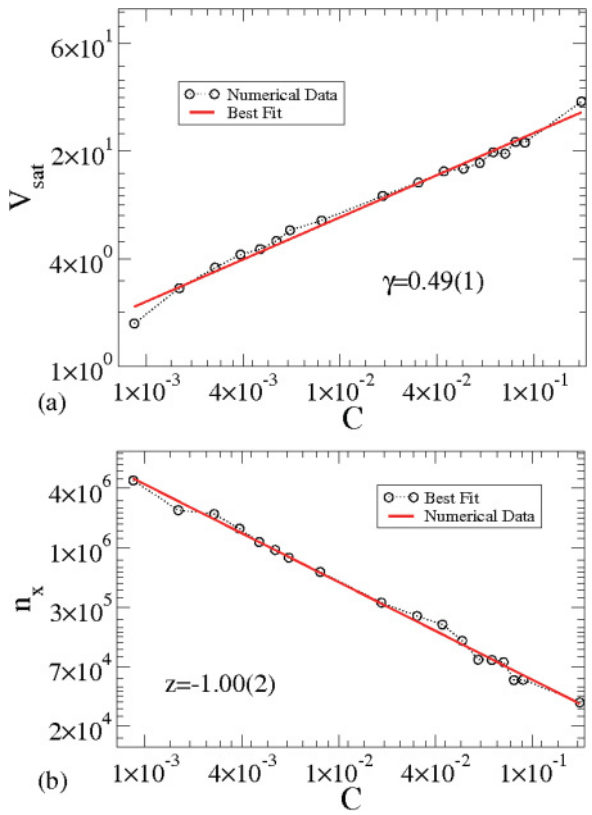

FIG. 5. (Color online) (a) Plot of V_{sat} as a function of the control parameter C. (b) Behavior of the crossover number n_x vs C.

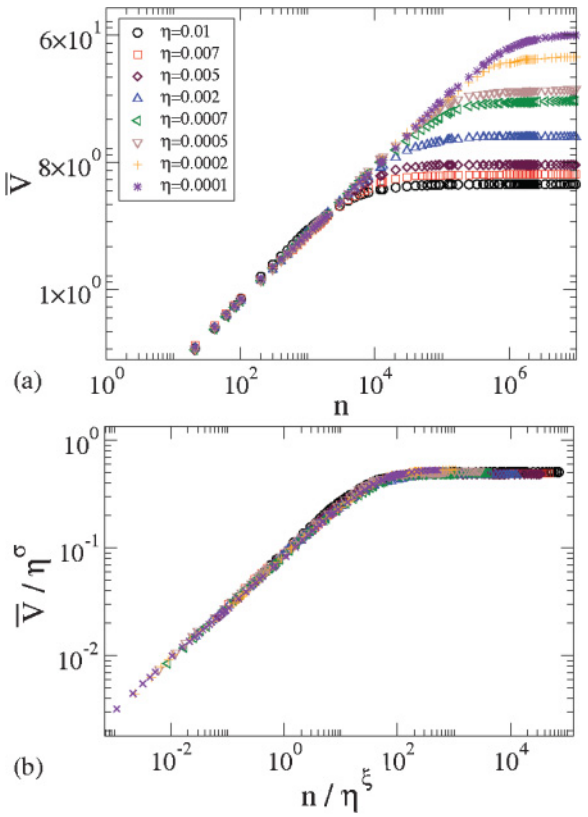

FIG. 6. (Color online) (a) Plot of the average velocity as a function of the number of collisions n for different values of the drag coefficient. (b) The collapse onto a single universal plot.

behaviors for short n. However, applying the transformation $n \to nC^2$ coalesces all the curves at short n, as shown in Fig. 4(b). For such behavior, we can also propose the following scaling hypotheses:

(1) When $n \ll n_x$ the average velocity is

$$\overline{V}(nC^2,C) \propto (nC^2)^{\beta}, \tag{8}$$

where the exponent β is called the acceleration exponent.

(2) When $n \gg n_x$, the average velocity is described as

$$\overline{V}_{\text{sat}} \propto C^{\gamma}, \tag{9}$$

where γ is the saturation exponent.

(3) The crossover from growth to saturation ($n \approx n_x$) is supposed to scale as

$$n_x \propto C^{z}, \tag{10}$$

where z is called the crossover exponent.

These scaling hypotheses, following the method of Leonel, McClintock and da Silva [35], allow us to describe the average velocity in terms of a scaling function of the type

$$\overline{V}(nC^2,C) = \lambda \overline{V}(\lambda^p nC^2, \lambda^q C), \tag{11}$$

where p and q are scaling exponents and λ is a scaling factor. Moreover, p and q must be related to β, γ, and z. Because λ is a scaling factor, we can specify that $\lambda^p nC^2 = 1$, yielding

$$\overline{V}(nC^2,C) = (nC^2)^{-1/p} \overline{V}_1(n^{-q/p}C), \tag{12}$$

where $\overline{V}_1[(nC^2)^{-q/p}C] = \overline{V}[1,(nC^2)^{-q/p}C]$ is assumed to be constant for $n \ll n_x$. Comparing Eqs. (8) and (12), we obtain $\beta = -1/p$. Now choosing $\lambda^q C = 1$, we find that $\lambda = C^{-1/q}$ and Eq. (11) is given by

$$\overline{V}(nC^2,C) = C^{-1/q} \overline{V}_2(C^{-p/q} nC^2), \tag{13}$$

where $\overline{V}_2(C^{-p/q}nC^2) = \overline{V}(C^{-p/q}nC^2,1)$ is assumed to be constant for $n \gg n_x$. Comparing Eqs. (9) and (13), we obtain $\gamma = -1/q$ [see Fig. 5(a)]. A power-law fitting in Fig. 4 gives us $\beta = 0.501(2)$. Such a value was obtained from the range $C \in [10^{-3}, 2 \times 10^{-1}]$. Given the two values of the scaling factor λ, and the condition for the crossover, $\lambda = (nC^2)^{-1/p} = (nC^2)^{\beta} = C^{-1/q} = C^{\gamma}$, one can easily conclude that $z = \frac{\gamma}{\beta} - 2 = -0.97(1)$, which is in excellent agreement with the values obtained numerically, as shown in Fig. 5(b). A confirmation of the initial hypotheses is made by the collapse of all the curves of $\overline{V}$ versus n onto a single and universal plot, as shown in Fig. 4(c), showing that the system is scaling invariant under specific transformations. With this good collapse of all the curves of the average velocity and considering that the critical exponents are $\beta \cong 0.5$, $\gamma \cong 0.5$, and $z \cong -1$, we can conclude that the time-dependent, dissipative, driven elliptical billiard belongs to the same class of universality as the one-dimensional (1D) nondissipative Fermi-Ulam model [35] and the periodically corrugated waveguide [36]. However, the physical reason for the saturation of the average velocity is quite different in the two cases. In the nondissipative case it is due to the existence of invariant curves, and in the dissipative case as studied in this

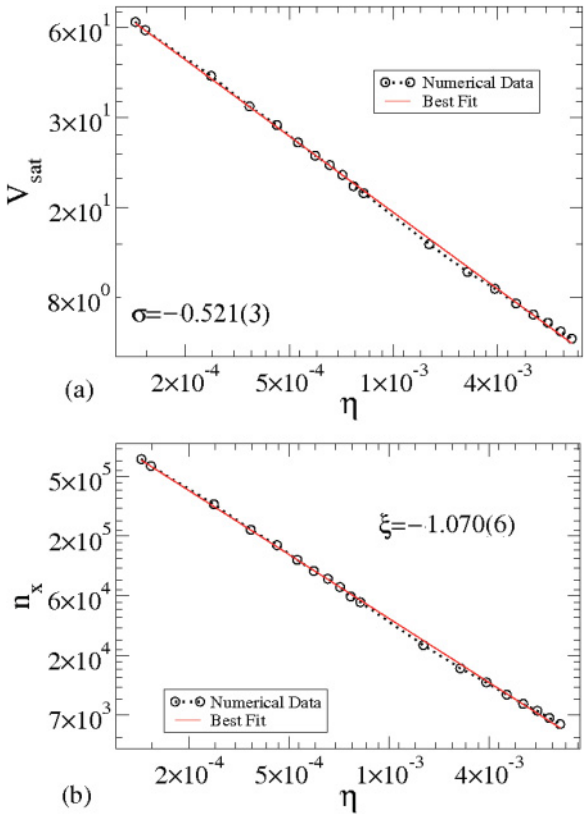

FIG. 7. (Color online) (a) Plot of V_{sat} as a function of the control parameter η. (b) Behavior of the crossover number n_x vs η.

paper it is due to dissipation. In the latter case attractors emerge in phase space onto which particles will be eventually captured, thus destroying unlimited diffusion, as also shown in [29]. The scaling can also be described in terms of the coefficient of the drag force η, as one can see in Fig. 6. In such a case, $V_{\rm sat} \propto \eta^{\sigma}$ and $n_x \propto \eta^{\xi}$, and $\sigma = -0.521(3)$ and $\xi = -1.070(6)$, as can be seen in Fig. 7. We have fixed $C = 0.1$ and $V_0 = 10^{-5}$. Therefore, $\eta \to 0$ implies that $V_{\rm sat}$ and n_x both diverge, thus recovering the results for the nondissipative case, i.e., exhibiting Fermi acceleration. Additionally, our results reinforce that in-flight dissipation is a sufficient condition to suppress the phenomenon of Fermi acceleration as in the case of collisional dissipation [28].

IV. CONCLUSION

We have studied some dynamical properties of a time-dependent elliptical driven billiard. In the static case, the system is integrable and two kinds of trajectories are observed: rotator and librator. We have introduced time-dependent perturbations and in-flight dissipation. We have observed that the average velocity grows for a small number of collisions, $n \ll n_x$, and then, after crossover $n \approx n_x$, it reaches a regime of saturation for large $n \gg n_x$. Thus we do not observe the unlimited energy growth (Fermi acceleration). We have also studied the behavior of the average velocity using scaling arguments. We have shown that there is a relation between the critical exponents γ, β, and z. Our scaling hypotheses are confirmed by a perfect collapse of all the curves onto a single universal plot. Additionally, we confirm that the two-dimensional dissipative elliptical model belongs to the same class of universality of the nondissipative Fermi-Ulam model (1D) and the corrugated waveguide (1D), for the range of the control parameters studied. The existence of power laws and the scaling property so far is established empirically and is thus an important open theoretical question.

ACKNOWLEDGMENTS

D.F.M.O is supported by the Slovenian Human Resources Development and Scholarship Program. M. R. acknowledges financial support from the Slovenian Research Agency (ARRS).

[1] G. Katz, M. A. Ratner, and R. Kosloff, Phys. Rev. Lett. **98**, 203006 (2007).
[2] S. E. Sklarz, D. J. Tannor, and N. Khaneja, Phys. Rev. A **69**, 053408 (2004).
[3] V. S. L'vov, A. Pomyalov, I. Procaccia, and V. Tiberkevich, Phys. Rev. Lett. **92**, 244503 (2004).
[4] P. Parmananda, M. Hildebrand, and M. Eiswirth, Phys. Rev. E **56**, 239 (1997).
[5] J. K. Bhattacharjee and D. Thirumalai, Phys. Rev. Lett. **67**, 196 (1991).
[6] M. N. Shneider and P. F. Barker, Phys. Rev. A **71**, 053403 (2005).
[7] R. Gommers, S. Bergamini, and F. Renzoni, Phys. Rev. Lett. **95**, 073003 (2005).
[8] M. Steiner, M. Freitag, V. Perebeinos, J. C. Tsang, J. P. Small, M. Kinoshita, D. Yuan, J. Liu, and P. Avouris, Nature Nanotechnol. **4**, 320 (2009).
[9] Y. Zhao, C. C. Ma, G. H. Chen, and Q. Jiang, Phys. Rev. Lett. **91**, 175504 (2003).
[10] W. V. Liu and W. C. Schieve, Phys. Rev. Lett. **78**, 3278 (1997).
[11] K. Tsumura and T. Kunihiro, Phys. Lett. B **668**, 425 (2008).
[12] H.-J. Stöckmann, *Quantum Chaos: An Introduction* (Cambridge University Press, Cambridge, England, 1999).
[13] C. Dembowski, H. D. Graf, A. Heine, T. Hesse, H. Rehfeld, and A. Richter, Phys. Rev. Lett. **86**, 3284 (2001).
[14] F. Libisch, C. Stampfer, and J. Burgdörfer, Phys. Rev. B **79**, 115423 (2009).
[15] M. F. Andersen, A. Kaplan, T. Grünzweig, and N. Davidson, Phys. Rev. Lett. **97**, 104102 (2006).
[16] E. Fermi, Phys. Rev. **75**, 1169 (1949).
[17] A. Loskutov, A. R. Ryabov, and L. G. Akinshin, J. Phys. A **33**, 7973 (2000).
[18] E. D. Leonel, D. F. M. Oliveira, and A. Loskutov, Chaos **19**, 033142 (2009).
[19] A. B. Ryabov and A. Loskutov, J. Phys. A **43**, 125104 (2010).
[20] D. F. M. Oliveira, J. Vollmer, and E. D. Leonel, Physica D **240**, 389 (2011).
[21] F. Lenz, F. K. Diakonos, and P. Schmelcher, Phys. Rev. Lett. **100**, 014103 (2008).
[22] J. Koiller, R. Markarian, S. M. O. Kamphorst, and S. P. de Carvalho, J. Stat. Phys. **83**, 127 (1996).
[23] D. F. M. Oliveira and E. D. Leonel, Phys. Lett. A **374**, 3016 (2010).
[24] D. F. M. Oliveira and E. D. Leonel, Physica A **389**, 1009 (2010).
[25] G. A. Luna-Acosta, Phys. Rev. A **42**, 7155 (1990).
[26] E. D. Leonel and P. V. E. McClintock, J. Phys. A **39**, 11399 (2006).
[27] E. D. Leonel and L. A. Bunimovich, Phys. Rev. E **82**, 016202 (2010).
[28] E. D. Leonel and L. A. Bunimovich, Phys. Rev. Lett. **104**, 224101 (2010).
[29] C. Petri, F. Lenz, F. K. Diakonos, and P. Schmelcher, Phys. Rev. E **82**, 035204(R) (2010).
[30] M. V. Berry, Eur. J. Phys. **2**, 91 (1981).
[31] Y. G. Sinai, *Introduction to Ergodic Theory* (Princeton University Press, Princeton, NJ, 1976).
[32] F. Lenz, F. K. Diakonos, and P. Schmelcher, Phys. Rev. E **76**, 066213 (2007).
[33] F. Lenz, C. Petri, F. R. N. Koch, F. K. Diakonos, and P. Schmelcher, New J. Phys. **11**, 083035 (2009).
[34] F. Lenz, C. Petri, F. K. Diakonos, and P. Schmelcher, Phys. Rev. E **82**, 016206 (2010).
[35] E. D. Leonel, P. V. E. McClintock, and J. K. Silva, Phys. Rev. Lett. **93**, 14101 (2004).
[36] E. D. Leonel, Phys. Rev. Lett. **98**, 114102 (2007).